

See discussions, stats, and author profiles for this publication at: <https://www.researchgate.net/publication/231656718>

# Interaction, Lipid Exchange, and Effect of Vesicle Size in Systems of Oppositely Charged Vesicles

ARTICLE *in* THE JOURNAL OF PHYSICAL CHEMISTRY · AUGUST 1996

Impact Factor: 2.78 · DOI: 10.1021/jp960327f

---

CITATIONS

43

---

READS

13

6 AUTHORS, INCLUDING:

[Valérie Marchi-Artzner](#)

French National centre for scientific research...

47 PUBLICATIONS 1,547 CITATIONS

SEE PROFILE



[Ludovic Jullien](#)

Ecole Normale Supérieure de Paris

137 PUBLICATIONS 3,021 CITATIONS

SEE PROFILE

## Interaction, Lipid Exchange, and Effect of Vesicle Size in Systems of Oppositely Charged Vesicles

Valérie Marchi-Artzner,<sup>†</sup> Ludovic Jullien,<sup>\*,†,‡</sup> Luc Belloni,<sup>§</sup> Danièle Raison,<sup>||</sup>  
Liliane Lacombe,<sup>†</sup> and Jean-Marie Lehn<sup>\*,†</sup>

Laboratoire de Chimie des Interactions Moléculaires, UPR 285, Collège de France, 11 Place Marcelin Berthelot, F-75231 Paris Cedex 05, France; Département de Chimie, URA 1679, Ecole Normale Supérieure, 24 rue Lhomond, F-75231 Paris Cedex 05, France; C.E.A.-Service de Chimie Moléculaire CE-Saclay, 91191-Gif-sur-Yvette, Cedex, France; and C.I.M.-Jussieu, Université Paris VI et VII, C.N.R.S., 7 quai Saint Bernard, 75252 Paris Cedex 05, France

Received: January 31, 1996; In Final Form: April 15, 1996<sup>®</sup>

The interactions between charged unilamellar vesicles of different size prepared from mixtures of egg lecithin (EPC<sup>1</sup>), cholesterol, and a charged component, either stearylamine or dicetyl phosphate, were investigated. Several techniques, i.e. fluorescence spectroscopy, <sup>133</sup>Cs-NMR, light scattering measurements, and electron and optical microscopies in dilute aqueous solutions, provided evidence that vesicles bearing opposite charges interact via contact followed by lipid exchange; the progressive charge neutralization is shown by <sup>133</sup>Cs-NMR to occur without fusion of vesicle internal pools. Vesicle size determines as diverse features as contact duration, extent of lipid exchange, and final distribution of surface charge among the vesicle mixture.

### Introduction

In living organisms, the lipid bilayer constitutes a basic unit that is involved in various fundamental processes such as control of solute permeability and osmotic balance, bioenergetics and metabolism, and cell–cell recognition.<sup>2</sup> Specific recognition between membrane surfaces is generally recognized to play a major role in cell adhesion or in the control of tissue growth.<sup>3</sup> Several types of mechanisms have been considered to account for this specificity, involving either specific protein–substrate interactions, diffusion of membrane-permeable solutes, or structural complementarity between bilayer surfaces covered by glycolipids and glycoproteins. To examine the significance of membrane surface on interbilayer interactions, experiments have been done with vesicles,<sup>4–7</sup> with force apparatus,<sup>8,9</sup> and on monolayers.<sup>10–13</sup> They emphasized the role of hydrophobic, Coulombic, and specific interactions that are also determining molecular recognition features.<sup>14</sup>

Vesicles represent suitable models of living cells as far as their membrane is concerned,<sup>15,16</sup> and several biological processes have been modeled in these artificial systems.<sup>12,17,18</sup> They are dynamically metastable organized assemblies that exhibit a rich behavior when submitted to external constraints.<sup>18,19</sup> Besides their basic interest, these features are especially important for the use of vesicles for drug delivery.<sup>20</sup> Regarding the latter, the investigation and the control of interactions between vesicles are of special significance.

Some of us have previously examined the transport of solutes through vesicle bilayers by shuttles<sup>21</sup> or channel-like molecules,<sup>22</sup> and the present paper reports studies on vesicle/vesicle recognition processes. In view of the richness of behavior that may be observed when two vesicles come into contact and of the biological relevance of this phenomenon, we have examined the consequences of the recognition features on collision, adhesion, or fusion between “complementary” vesicles. To set

up our experimental protocol, we first considered mixtures of positively and negatively charged vesicles.<sup>23,24</sup> Such studies are biologically significant since cell membranes generally exhibit net negative surface charge. Consequently, Coulombic interactions could offer strategies for drug delivery. Furthermore, positively charged lipids are increasingly used as gene delivery vectors for gene therapy, and a full understanding of their mechanism of action is crucial for controlling and optimizing the membrane crossing.

### Results and Discussion

**Structure and Lipid Composition of the Vesicles.** Many charged lipids give vesicles under various preparation conditions.<sup>25</sup> Unfortunately, the vesicles prepared from such lipids, e.g. cetyl phosphate and DODAB, are sensitive to many parameters such as pH and ionic strength, and they display complicated behaviors such as aggregation and fusion that might make difficult the interpretation of experiments done on mixtures of positively and negatively charged vesicles.<sup>26–28</sup> To decrease the intrinsic sensitivity of the initial preparations of identically charged vesicles, we chose to work with commercially available mixtures containing egg phosphatidylcholine (EPC) as the major component (70 mol %), cholesterol (10 mol %), and dicetyl phosphate or stearylamine (20 mol %), respectively, as negatively or positively charged components (CC). The former lipid mixture is about the same as that found in many membranes of mammalian cells. Vesicles were essentially prepared by detergent dialysis (DD).<sup>29</sup> Sonication and the reverse phase methods have also been occasionally used to respectively obtain small vesicles (SUV)<sup>30</sup> and large vesicles (REV).<sup>31</sup> Dynamic light scattering showed the average diameters of the DD vesicles to be 70 and 100 nm for the positively and negatively charged vesicles, respectively (Table 1). Furthermore, the analysis of the data showed the positively charged vesicles to be more polydisperse than the negatively charged ones. However, electron microscopy indicated that DD vesicles prepared from either positive or negative lipid sets were unilamellar and rather polydisperse with no clear difference between both types of vesicles. In the present case, dynamic light scattering data provide the most reliable size estimate since electron microscopy

<sup>†</sup> Collège de France.

<sup>‡</sup> Ecole Normale Supérieure.

<sup>§</sup> C.E.A.-Service de Chimie Moléculaire.

<sup>||</sup> C.I.M.-Jussieu.

<sup>®</sup> Abstract published in *Advance ACS Abstracts*, July 1, 1996.

**TABLE 1: Radii of LUV Prepared by Detergent Dialysis As Measured by Static and Dynamic Light Scattering**

	vesicle radius $\pm 5$ (nm) <sup>a</sup>	vesicle radius $\pm 5$ (angle) (nm) <sup>b</sup>
positively charged vesicles, +		
2 mg/mL	77	34 (90°)
1 mg/mL	77	37 (60°)
0.25 mg/mL	67	
negatively charged vesicles, -		
2 mg/mL	50	50 (90°)
1 mg/mL	53	50 (60°)
0.25 mg/mL	56	
+/- 1/1		
2 mg/mL	50	36 (90°)
1 mg/mL	48	
0.25 mg/mL	52	

<sup>a</sup> Measured by static light scattering at angles from 50° to 130° (extracted from the Guinier plot). <sup>b</sup> Measured by dynamic light scattering at different angles.

**TABLE 2: Chemical Yields of Formation and Lipid Composition of Bilayers for Vesicles Prepared by Detergent Dialysis (See Experimental Section)**

nature of lipid mixture	positive	negative
yield of vesicle formation $\pm 10$ (%) <sup>a</sup>	100	100
yield of vesicle formation $\pm 10$ (%) <sup>b</sup>	100	100
composition EPC/Chol/CC $\pm 5$ (%) <sup>c</sup>		
before vesicle formation	70/10/20	70/10/20
after vesicle formation	70/10/20	70/10/20

<sup>a</sup> Obtained by phosphorus titration and based on phosphorus-containing components. <sup>b</sup> Obtained by quantitative TLC and based on egg lecithin. <sup>c</sup> Obtained by quantitative TLC and based on egg lecithin.

histograms were based on statistics done on a limited number of vesicles, whereas dynamic light scattering experiments take into account a much larger number of vesicles. All vesicle preparations were shown to be structurally stable for at least 1 week according to our physicochemical methods.

The yield of DD vesicles together with the determination of lipid composition before and after vesicle formation was estimated by a phosphorus assay<sup>32</sup> and by quantitatively measuring the concentration of lipid components after analytical thin layer chromatography (TLC). Both investigations showed vesicle formation to be essentially quantitative (Table 2). Furthermore, the TLC investigation demonstrated the ratios between the components of the lipid mixture to be conserved after dialysis (EPC/Chol/CC 70/10/20). No trace of octyl- $\beta$ -glucopyranoside, detergent used for preparing vesicles, was detected by TLC in final preparations of vesicles.

Thus positively and negatively charged unilamellar vesicles have been prepared. Their chemical composition has been accurately determined, and the structural analysis emphasized both a significant difference of average diameter and polydispersity between both vesicle populations.

**Lipid Exchange between Oppositely Charged Vesicles.** Fluorescence spectroscopy is a widely used technique for studying organized assemblies.<sup>25,33</sup> For vesicular systems, it provides sensitive methods to analyze diverse processes such as lipid phase transition and coalescence phenomena such as vesicle aggregation, lipid exchange, and vesicle fusion.

A first experiment was done to examine whether any interaction took place when positively and negatively charged vesicles were mixed. It was based on resonance energy transfer (RET) between NBD-PE,<sup>1</sup> acting as the energy donor, and Rh-PE,<sup>1</sup> acting as the energy acceptor.<sup>25,33</sup> Aliquots of a 10 mM glucose solution of positively charged vesicles containing 1 mol % Rh-PE (Rh+; 5 mM) were progressively added into a 10

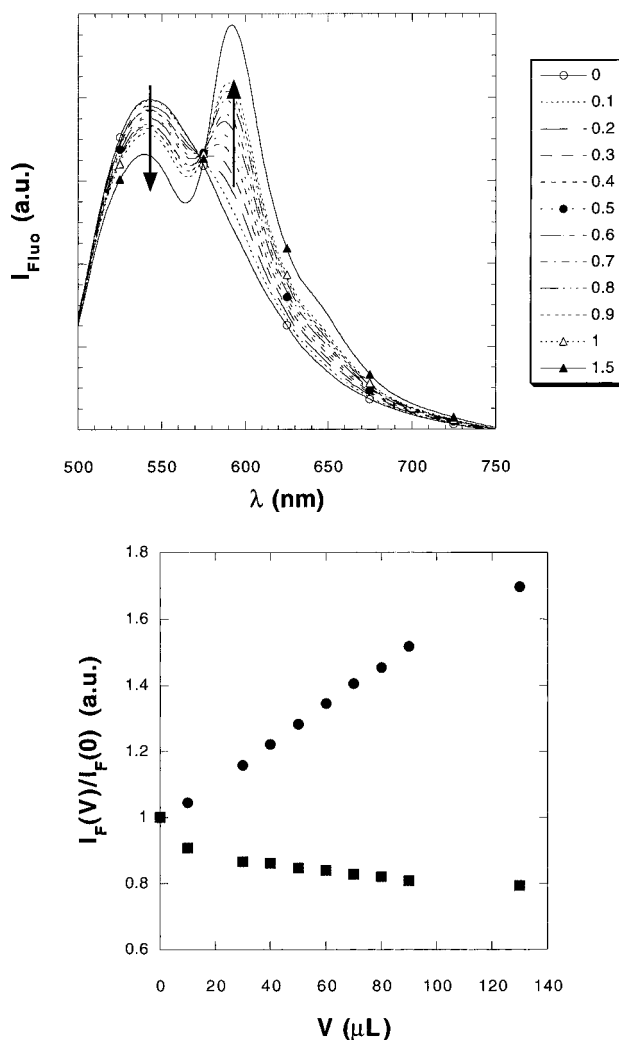


**Figure 1.** (a, top) Fluorescence emission spectra arising from titration of 3 mL of 220  $\mu$ M 1 mol % NBD-PE negatively charged vesicles (NBD-) in 10 mM glucose by a solution of 5 mM 1 mol % Rh-PE positively charged vesicles (Rh+) in 10 mM glucose ( $\lambda_{exc} = 460$  nm). (b, bottom) Normalized fluorescence intensity  $I_F(V)/I_F(0)$  arising from titration of 3 mL of 220  $\mu$ M 1 mol % NBD-PE negatively charged vesicles (NBD-) in 10 mM glucose as a function of the volume  $V$  of the solution of 5 mM 1 mol % Rh-PE positively charged vesicles (Rh+) in 10 mM glucose (see the Experimental Section). Squares: NBD fluorescence ( $\lambda_{exc} = 460$  nm;  $\lambda_{em} = 543$  nm). Circles: Rh fluorescence ( $\lambda_{exc} = 460$  nm;  $\lambda_{em} = 589$  nm). Errors on volumes and ratios of fluorescence intensities are inferior to the marker dimensions.

mM glucose solution of negatively charged vesicles containing 1 mol % NBD-PE (NBD-; 220  $\mu$ M). Figure 1a displays the fluorescence spectra in the course of the titration, whereas Figure 1b shows the evolution of fluorescence emission from NBD or from Rh. During titration, the NBD fluorescence decreases asymptotically, whereas the emission of Rh increases almost linearly. Upon consideration that vesicles are still present, as evidenced by light scattering and electron microscopy, such a fluorescence behavior is in agreement with an increase of energy transfer between NBD-PE and Rh-PE. In the absence of an inner filter effect as in the present case, this observation is accounted for by a decrease of the average distance between donor and acceptor probes. For Rh-PE, the linearly increasing emission arising from direct excitation overcomes the expected decreasing RET contribution. In the case of identically charged vesicles, no attractive interaction was detected: the behavior expected from dilution was observed when dye-labeled, identically charged vesicles were mixed.

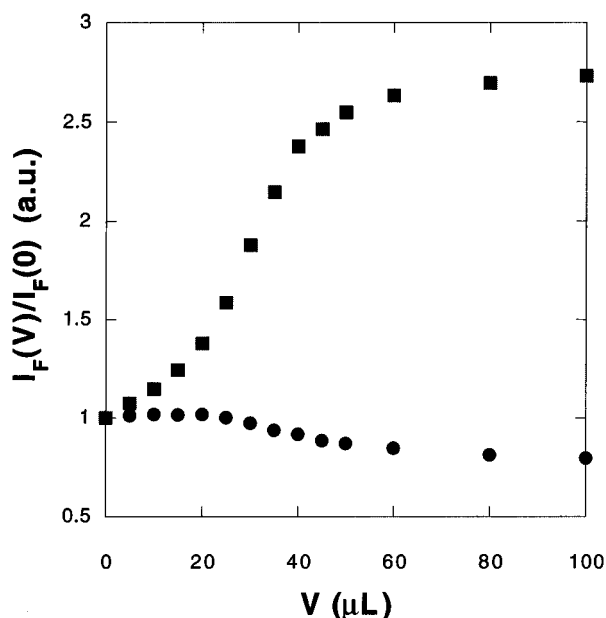


**Figure 2.** Normalized fluorescence intensity  $I_F(V)/I_F(0)$  arising from titration of 2.5 mL of 67  $\mu\text{M}$  0.75 mol % NBD-PE and 0.75 mol % Rh-PE negatively charged vesicles (NBD/Rh-) in 10 mM glucose as a function of the volume  $V$  of the solution of 5 mM unlabeled positively charged vesicles (+) in 10 mM glucose (see the Experimental Section). Squares: NBD fluorescence ( $\lambda_{\text{exc}} = 460$  nm;  $\lambda_{\text{em}} = 543$  nm). Circles: Rh fluorescence ( $\lambda_{\text{exc}} = 460$  nm;  $\lambda_{\text{em}} = 589$  nm). Errors on volumes and ratios of fluorescence intensities are inferior to the marker dimensions.

A new experiment was then performed to provide information about which process, aggregation or lipid exchange, was taking place between oppositely charged vesicles. A 10 mM glucose solution of negatively charged vesicles containing 0.75 mol % NBD-PE and 0.75 mol % Rh-PE (NBD/Rh-; 40  $\mu\text{M}$ ) was titrated with a 10 mM glucose solution of unlabeled positively charged vesicles (+; 5 mM). As shown in Figure 2, the RET monitored either by emission of NBD ( $\lambda_{\text{em}} = 540$  nm) or of Rh ( $\lambda_{\text{em}} = 590$  nm) under NBD excitation ( $\lambda_{\text{exc}} = 460$  nm) continuously decreased during titration until equivalence, defined as the point where identical numbers of moles of oppositely charged components were present in the mixture.<sup>34</sup> After equivalence, the fluorescence emission remained constant. This behavior is in line with the diffusion and exchange of both fluorescent probes between both types of vesicles.

Furthermore, the fluorescence signals remained stable in time after each addition, suggesting that interaction between oppositely charged vesicles occurred in less than 10 s, whereas no change in fluorescence signals occurred in more than 1 h in the case of identically charged vesicles.

On the time scale of observation, this set of experiments demonstrate that positively and negatively charged vesicles interact attractively in aqueous solution, whereas identically charged ones do not. This interaction results in exchange of lipids and does not manifest itself only as an adhesion between the vesicles.

**Oppositely Charged Vesicles Exchange Membrane Components: Second Set of Fluorescence Experiments.** The first experiments directly supporting the lipid exchange were completed by a new set of fluorescence experiments. In the present system, any lipid exchange should yield a change of the surface charge of the membrane. This evolution could either modify the properties of a membrane-incorporated probe or affect the membrane adsorption of a charged probe displaying environment-dependent properties.

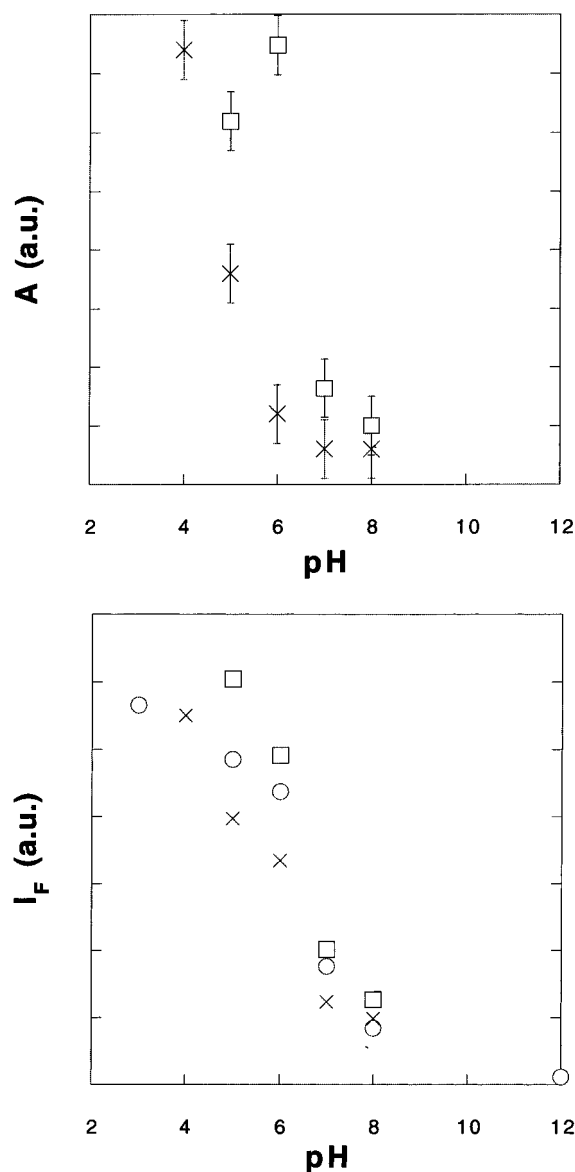


**Figure 3.** Influence of pH of the surrounding aqueous solution on Rh-PE absorbance  $A$  (a, top) and fluorescence emission  $I_F$  ( $\lambda_{\text{exc}} = 560$  nm;  $\lambda_{\text{em}} = 590$  nm) (b, bottom) in different bilayer environments (times signs, 20 mol % positively charged vesicles; circles, EPC vesicles; squares, 20 mol % negatively charged vesicles). Lipid concentration: 5 mg/mL in Britton-Robinson buffers at several pH's at constant 0.1 M ionic strength. Errors on ratios of fluorescence intensities are inferior to the marker dimensions.

Since only proton and hydroxide ions are present in aqueous glucose solution, pH-sensitive probes were searched to sense the membrane charge. The NBD chromophore is pH-independent and should not exhibit major alterations of absorption and emission features when changing the pH. On another hand, the Rh chromophore is a diacid and is expected to display an evolution of its spectroscopic properties with the protonation state.

In a first assay, small neutral EPC and positively and negatively charged vesicles labeled with Rh-PE were prepared by sonication in different buffer solutions<sup>35</sup> (ionic strength 0.1 M<sup>36</sup>). UV-visible absorption and fluorescence emissions of the vesicle suspensions were recorded (Figure 3a,b). All vesicle preparations exhibited a sharp decrease of Rh-PE absorption and fluorescence emission when going from low pH to high pH with an inflexion at about  $\text{pH} \approx 6.5$ . The Rh-PE molar absorption coefficient at 560 nm and fluorescence emission ( $\lambda_{\text{exc}} = 560$  nm,  $\lambda_{\text{em}} = 590$  nm) in basic solutions were respectively

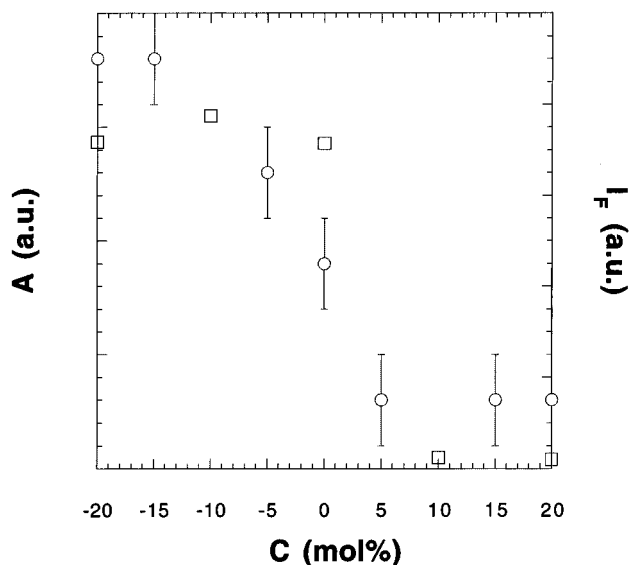


**Figure 4.** Influence of the surface charge of the lipid membrane on Rh-PE absorption (circles; absorbance  $A$  at 560 nm) and fluorescence emission  $I_F$  (squares;  $\lambda_{exc} = 560$  nm;  $\lambda_{em} = 590$  nm). Lipid concentration: 5 mg/mL in 10 mM glucose. [Rh-PE]/[lipid mixture] = 0.15%. Errors on volumes and ratios of fluorescence intensities are inferior to the marker dimensions.

about one-third and one-fifth of that in acidic ones. Compared to EPC vesicles, the position of the drops of absorption and fluorescence emission was shifted toward lower (respectively higher) pH values for positively (respectively negatively) charged vesicles. The observation of a change in Rh-PE absorption and fluorescence emission around pH = 6.5 reasonably agrees with reported values for free rhodamine.<sup>37</sup> The observation of different shifts of the apparent Rh  $pK_a$  according to the membrane charge is in agreement with the expectations: when the lipid surface is positively (respectively negatively) charged, ionization of the acid group is facilitated (respectively disfavored), leading to a lower (respectively higher) apparent  $pK_a$ .

In a second assay, vesicles containing various percentages of charged lipids and 0.15 mol % of NBD-PE or Rh-PE (lipid concentration: 5 mg/mL; 7 mM) in 10 mM glucose were prepared by mixing appropriate amounts of the charged kits and EPC. NBD absorption and fluorescence emission spectra were not affected by the membrane composition. In contrast, Rh-PE spectra dramatically changed but did not essentially depend on the molar fraction of charged additives contained in the bilayer (Figure 4). This behavior agrees with the already invoked charge effect of the membrane surface. Interestingly, since the bulk pH of unbuffered vesicle suspensions is almost equal to the Rh  $pK_a$ , even a small change of membrane "charge" around neutrality is strongly reflected in UV-visible absorption and fluorescence emission of Rh-PE.

The possible modulation of the Rh-PE spectroscopic properties addresses the issue whether the interpretation of the NBD/Rh RET evolution in terms of distance is still valid in the present system. Indeed, RET should be affected by a modification of the NBD/Rh Förster radius that depends on the molar absorption coefficient  $\epsilon$ (Rh-PE). For both RET experiments displayed on Figures 1b and 2, the variations of the average NBD/Rh distance and of  $\epsilon$ (Rh-PE) act in the same direction to modify the efficiency of RET. Consequently, the conclusions arising from RET experiments are not modified by taking into account Rh-PE features.

Taking advantage of the Rh-PE ability to sense membrane "charge", complementary fluorescence studies were performed

by following only the Rh-PE behavior. Several titrations between unlabeled vesicles and vesicles containing 0.15 mol % Rh-PE were investigated: (A/B: titration of A by B) +/Rh-; Rh-/+; -/Rh+; Rh+/- . Figure 5a-d displays the evolution of the Rh-PE fluorescence emission during the corresponding titrations together with the simulation of the expected evolution under the assumption that no vesicle interaction occurs.<sup>38</sup> Several points common to all these titrations can be made: (i) a deviation from the behavior without interaction is always present, confirming the RET investigations; (ii) the titration curves emphasize the significance of the equivalence, after which the deviation is stabilized; (iii) before equivalence, three basic titration curves obtained by the difference between experimental titration curves and calculated ones under assumption of noninteraction have been observed, i.e., linear for Rh-/+ (Figure 5b); sigmoidal for +/Rh- (Figure 5a) and for Rh+/- (Figure 5d); and non-monotonous for -/Rh+ (Figure 5c).

To confirm the preceding observations related to the change of membrane charge during the titrations, we repeated these titrations in the presence of 2-(*p*-toluidino)naphthalene-6-sulfonic acid (TNS), a classical anionic probe that directly senses membrane surface potential by the environmental modulation of its fluorescence.<sup>39</sup> We first studied the influence of the surface charge of the lipid membrane on TNS fluorescence by adding vesicles bearing various amounts of charged lipids (50  $\mu$ L; lipid concentration 5 mg/mL) to  $10^{-7}$  M TNS aqueous solutions. TNS fluorescence was strongly enhanced in the presence of positively charged vesicles, in agreement with the literature<sup>39</sup> (data available in the supporting information). Then we examined the titrations +/- (respectively -/+) of unlabeled positively (respectively negatively) charged vesicles by negatively (respectively positively) charged ones in a  $10^{-7}$  M TNS aqueous solution (data available in the supporting information). They confirm the trend observed in Rh-PE sensed titrations: (i) there is a deviation of the experimental behavior from the expected one assuming that no interaction occurs, the deviation being maximal at equivalence; (ii) after equivalence, the fluorescence signal tends toward the curve expected without interaction in the -/+ titration, whereas it remains almost constant in the +/- titration; (iii) at equivalence, the surface potential of the vesicles corresponds to a surface potential intermediate between that of the initial and titrating vesicles.

Rh-PE and TNS titrations thus confirmed and precise RET experiments by showing that the lipid exchange occurring between oppositely charged vesicles was associated with a reduction of the surface charge of the bilayers. In line with previous studies,<sup>23</sup> these results suggest that charged membrane components exchange between oppositely charged vesicles.

**<sup>133</sup>Cs-NMR Experiments as a Tool To Reveal the Absence of Fusion of Internal Pools between Interacting Vesicles.** The preceding experiments do not give any information on whether or not lipid exchange is accompanied by vesicle fusion with mixing of internal vesicle pools. To this end, two common assays for characterization of vesicle fusion were performed. For both terbium (III)/dipicolinic acid<sup>40</sup> and cobalt (II)/calcein systems,<sup>41</sup> no change of fluorescence emission was observed when vesicles of opposite charge containing the system components were mixed (see the Experimental Section). Unfortunately, at the concentrations used, it was impossible to control the validity of these assays; addition of Triton X-100 destroys vesicles, but it also promotes a high dilution (from 10  $\mu$ L to 3 mL), which decreases considerably the complex formation that constitutes the basis of such assays. Consequently, although they might indicate that no vesicle fusion took place between

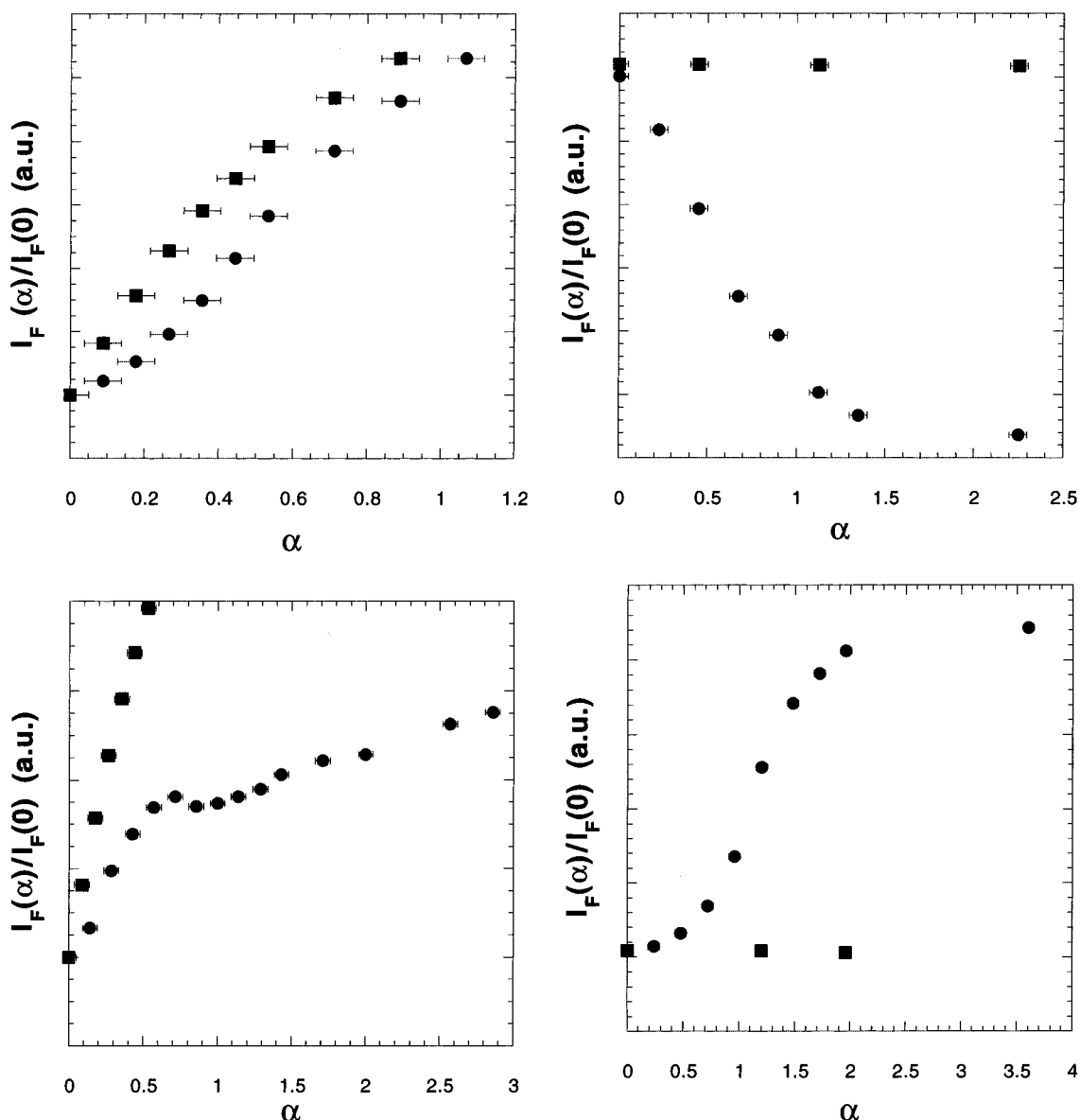


**Figure 5.** Evolution of fluorescence emission of Rh-PE in the course of titrations A/B<sup>34</sup> (circles; A/B, titration of A by B;  $\lambda_{exc} = 560$  nm;  $\lambda_{em} = 589$  nm) together with the simulation of the evolution of the fluorescence of Rh-PE under the assumption that no vesicle interaction occurs (squares). [Rh-PE]/[lipid mixture] = 0.15%; lipid concentration, 3.4 mg/mL in glucose 10 mM; (a, top left) +Rh-; (top, right) Rh-/+; (bottom, left) -Rh+; (bottom, right) Rh+/- . Errors on volumes and ratios of fluorescence intensities are inferior to the marker dimensions.

vesicles of opposite charges, we decided to design a new assay to detect vesicle fusion with a better control reliability.

Alkali metal NMR has proven to be a valuable tool to investigate vesicle features or to sense lipid environments.<sup>42,43</sup> Among nuclei that have already been used for this purpose, <sup>133</sup>Cs is probably one of the most attractive due to its isotopic abundance, narrow signals, large range of chemical shifts, and high sensitivity to environmental effects.<sup>44</sup> In aqueous solution, the chemical shift of <sup>133</sup>Cs<sup>+</sup> strongly depends on ion concentration.<sup>45</sup> The latter feature led us to consider a fusion assay based on mixing vesicle populations containing Cs<sup>+</sup> solutions of different concentrations and monitoring the signals arising from the mixed solution. Any leakage, breakage, or fusion should give new NMR signals, the chemical shifts of which are reminiscent of the processes that gave rise to them.

The chemical shifts of isoosmolar aqueous CsCl/glucose solutions (osmolarity = 100 mOsm) were first recorded. Figure 6a displays the dependence of the <sup>133</sup>Cs-NMR chemical shift of Cs<sup>+</sup> cations on CsCl concentration at 20 °C (reference in an external tube: 10.7 mM CsCl in D<sub>2</sub>O). This dependence can be satisfactorily described as linear in the range of investigated

concentrations ( $\delta$  (ppm) = 1.14 + 12.6[CsCl](M)). Nevertheless, it seems reasonable to assume that the linear dependence does not apply at low concentrations when ion-ion interactions involved in the shifting of signals become negligible. At a concentration lower than 10 mM, the present calibration suggests that the chemical shift of <sup>133</sup>Cs<sup>+</sup> cations remains equal to 1.18 ± 0.04 ppm.

Positively and negatively charged DD vesicles were respectively prepared in aqueous CsCl 50 mM and in a mixture of CsCl 20 mM and glucose 60 mM (lipid concentration: 20 mg/mL). Each vesicle preparation was extensively dialyzed against 100 mM glucose in order to remove all external Cs<sup>+</sup> ions. Aliquots of each vesicle suspension were then mixed, and the <sup>133</sup>Cs-NMR spectra were recorded. Figure 6b displays <sup>133</sup>Cs-NMR spectra from different mixtures, and Table 3 summarizes the results. The positively charged vesicles gave rise to one slightly asymmetrical signal at  $\delta = 1.71$  ppm, whereas no signal was visible from the negatively charged vesicles. For mixtures of both vesicle suspensions, two peaks sharing identical longitudinal relaxation times  $T_1 \approx 10$  s were observed at  $\delta = 1.71$  ppm and  $\delta = 1.18$  ppm.

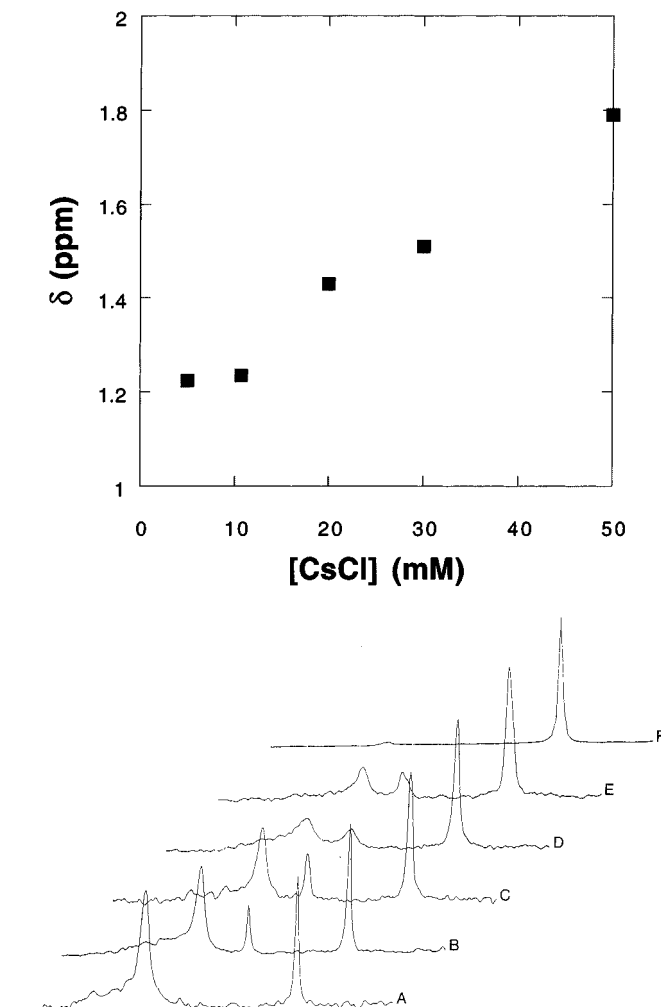


**Figure 6.** (a, top)  $^{133}\text{Cs}$ -NMR chemical shift  $\delta$  in ppm in isoosmolar solutions of CsCl and glucose (external reference: 10.7 mM CsCl in  $\text{D}_2\text{O}$ ); errors on concentrations and chemical shifts are inferior to the marker dimensions. (b, bottom)  $^{133}\text{Cs}$ -NMR spectra resulting from mixing of positively charged vesicles (+; prepared in CsCl, 50 mM) and negatively charged vesicles (-; prepared in CsCl, 20 mM, and glucose, 60 mM) (external reference: 10.7 mM CsCl in  $\text{D}_2\text{O}$ ): (A) 1.8 mL +, (B) 1.4 mL +/0.4 mL -; (C) 1.05 mL +/0.75 mL -; (D) 0.75 mL +/1.05 mL -; (E) 0.4 mL +/1.4 mL -; (F) 1.8 mL -;  $T = 293 \pm 1$  K.

Consider first the behavior of pure vesicle suspensions. For positively charged vesicles, the preceding calibration gives  $46 \pm 5$  mM for the internal  $\text{Cs}^+$  concentration, which is in good agreement with the 50 mM initial value. Only marginal cation loss, if any, occurred during the washing step of vesicle preparation. The absence of any visible signal for the preparation of negatively charged vesicles can be explained by considering that (i) chemical shifts as large as hundreds of ppm have been reported for external cesium cations when changing the membrane surface charge of vesicles;<sup>42</sup> and (ii) condensation of  $\text{Cs}^+$  cations occurs close to negatively charged surfaces; this effect causes an inhomogeneity of the chemical shifts of the ions and introduces a factor of signal broadening.<sup>46</sup> For the negatively charged vesicles, the width of the NMR signal is presumably too large to be visualized against the noise background.

For vesicle mixtures, the issue of fusion can be addressed by observation either of chemical shifts or of peak integrals. In the case of fusion, one expects to observe three peaks: two corresponding to the initial vesicles and another arising from fused vesicles. Due to the monotonous dependence of chemical shifts on concentration, the latter peak should be located between

the two former signals. In the present case, a new peak was indeed observed when negatively and positively charged vesicles were mixed, but its chemical shift (1.18 ppm) did not correlate by far with the chemical shift expected for fusion between vesicles of the same size range.<sup>47</sup> Consequently,  $^{133}\text{Cs}$ -NMR experiments demonstrate that there is no mixing of internal vesicular compartments when positively and negatively charged vesicles are mixed.

To complement the preceding NMR experiments, the possible consequences of vesicle mixing on size and shape distribution in the vesicle population have been also tentatively analyzed by light scattering (Table 1) and electron microscopy. No large size change was ever observed, but the difference of vesicular diameters and polydispersity between the two populations obscures the analysis of the data and forbids the unambiguous detection of fusion events by these methods. Nevertheless, these experiments demonstrated the absence of long-term adhesions or considerable aggregation between oppositely charged vesicles.

Electron microscopy and light scattering thus confirmed  $^{133}\text{Cs}$ -NMR observations: under the present conditions, no fusion between internal pools of vesicles was observed when negatively and positively charged vesicles were mixed. Furthermore, these techniques showed that the lipid exchange in LUV was not associated to any long-term or large-scale vesicle aggregation. The present result on LUV is in line with a previous report that nevertheless mentioned the occurrence of some aggregation between oppositely charged vesicles.<sup>23</sup> The lack of aggregation in our system could be linked to the kinetics of lipid exchange. In the present case, the single-chain stearylamine should exchange faster than the quaternary ammonium used in previous studies<sup>23</sup> and thus forbids the observation of large vesicle aggregates.

**Mechanism of Lipid Exchange between Positively and Negatively Charged Vesicles.** Two basic mechanisms of lipid exchange may be considered in order to account for the present experimental results. In the first mechanism (Figure 7a), lipid exchange occurs directly via the aqueous medium either by diffusion of individual membrane components or by diffusion of micelles formed from one vesicle bilayers. In the second one (Figure 7b), adhesion between vesicles bearing opposite charges constitutes the first event, which is then followed by a local lipid exchange process.

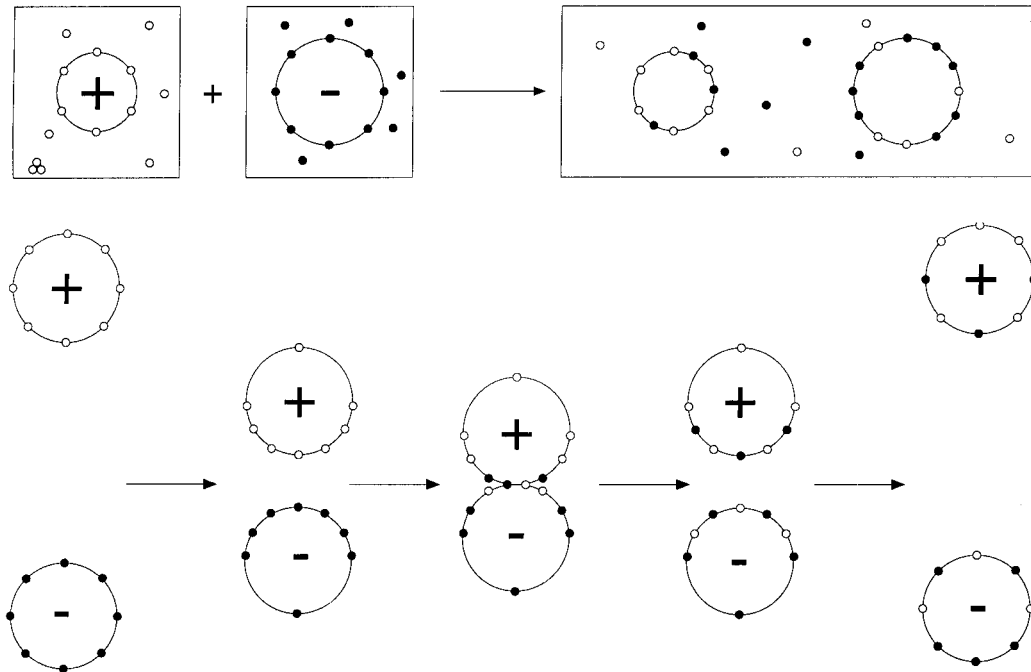
To assess which mechanism is preferentially acting in the present system, the order of magnitude of the exchange rates was first estimated. Let us first examine the compatibility of the observed lipid exchange rates with scheme a and then scheme b. An indication can be found in the exit rate constant of lipid components for vesicles with a membrane in the liquid-crystalline state at room temperature. When pyrenenonanoic acid was used as the exchanged molecule between DMPC vesicles at 28 °C, exit rate constants ranging from 0.1 to 5  $\text{s}^{-1}$  were observed at pH = 2.8 and 7.4, respectively.<sup>48</sup> These values can be assumed to lie in the range of the exit rate constants of stearylamine in positively charged vesicles. Reported exit rate constants for two alkyl chains lipids are much lower.<sup>49</sup> This suggests that during our observation on mixtures between oppositely charged vesicles only stearylamine could be exchanged between vesicles in order to reach an equilibrium state in less than 10 s, the other two alkyl chains components (in particular the two fluorescent probes NBD-PE and Rh-PE) exchanging too slowly to be reasonably involved in the lipid exchange process.<sup>50</sup>

As far as the kinetics of lipid exchange associated with scheme b is concerned, a lower limit of the exchange rate can be calculated by assuming that the rate is controlled by diffusion

**TABLE 3: Parameters Extracted from  $^{133}\text{Cs}$ -NMR Spectra Recorded from Mixtures of positively Charged Vesicles (+; Prepared in CsCl, 50 mM) and Negatively Charged Vesicles (-; Prepared in CsCl, 20 mM, and Glucose, 60 mM) (External Reference: 10.7 mM CsCl in  $\text{D}_2\text{O}$ );  $T = 293 \pm 1$  K**

volume of vesicles (mL)						
$V_+$	1.8	1.4	1.05	0.75	0.4	0
$V_-$	0	0.4	0.75	1.05	1.4	1.8
chemical shifts $\delta \pm 0.04$ (ppm)						
	1.81	1.81	1.76	1.77	1.73	<i>a</i>
	<i>a</i>	1.23	1.21	1.25	1.26	<i>a</i>
longitudinal relaxation time $T_1 \pm 1.5$ (s)						
$\delta = 1.71$ ppm	10	10	8	9	<i>b</i>	<i>a</i>
$\delta = 1.18$ ppm	<i>a</i>	10	12	9	<i>b</i>	<i>a</i>
linewidth at half-height $\pm 1$ (Hz)						
$\delta = 1.71$ ppm	3	3	4	3	<i>b</i>	<i>a</i>
$\delta = 1.18$ ppm	<i>a</i>	1	2	1	<i>b</i>	<i>a</i>
normalized areas $A$ of signals ( $\pm 20\%$ )						
$A_+$ ( $\delta = 1.71$ ppm) <sup>c</sup>	340	250	160	120	70	<i>a</i>
$A_-$ ( $\delta = 1.18$ ppm) <sup>d</sup>	<i>a</i>	35	40	35	30	<i>a</i>
$A_0$ ( $\delta = 0$ ppm)	100	100	100	100	100	100
corrected integrals $\mathcal{A}$ of signals						
$\mathcal{A}_+$ ( $\pm 20$ ) <sup>e</sup>	320	255	190	120	60	0
$\mathcal{A}_-$ ( $\pm 10$ ) <sup>f</sup>	0	20	40	60	80	100
$\inf(V_+, V_-)/V_-$	1	1	1	0.7	0.3	0
$A_-/A_+$	1	1.7	1	0.6	0.4	0

<sup>a</sup> No signal. <sup>b</sup> Not enough precision. <sup>c</sup> Integration from 3.70 to 1.49 ppm. <sup>d</sup> Integration from 1.45 to 0.61 ppm. <sup>e</sup> Obtained from linear regression of  $A_+$  as a function of  $V_+$ . <sup>f</sup> Obtained from  $\mathcal{A}_+$  after taking into account the differences of internal concentrations ( $[\text{Cs}^+]_+ = 46$  mM;  $[\text{Cs}^+]_- = 10$  mM) and vesicular sizes (all other things being equal, the internal compartmented volume in positively charged vesicles is 0.7 times smaller than the internal compartmented volume in negatively charged vesicles) between positively and negatively charged vesicles;  $\mathcal{A}_- = 0.31 \mathcal{A}_+$ .

**Figure 7.** Possible mechanisms of lipid exchange between vesicles: (a, top) by diffusion of free or associated membrane components; (b, bottom) by adhesion between interacting vesicles followed by a local lipid exchange.

of vesicles toward each other. A crude order of magnitude can be obtained by applying the following expression giving the number  $G$  of collisions per unit of time for a given vesicle in the mixture of interacting spherical vesicles:<sup>51</sup>

$$G = 8\pi D_i n_0 \int_{2R_1}^{+\infty} \frac{1}{r^2} e^{\varphi_{12}/kT} dr$$

with

$$\varphi_{12} = \frac{z_1 z_2 e^{-\kappa r}}{4\pi\epsilon_0\epsilon_r(1 + \kappa R_1)(1 + \kappa R_2)r}$$

and

$$D_i = \frac{kT}{6\pi\eta R_i}$$

where  $D_i$  is the diffusion coefficient,  $R_i$  is the radius,  $n_0$  is the concentration of the interacting vesicles,  $\eta$  is the viscosity, and  $\kappa^{-1}$  is the Debye–Hückel reciprocal length of the solution. Under the assumption that the vesicles are identical but bearing opposite charges and taking  $\eta = 10^{-3}$  Pa s,  $R_1 = R_2 = R = 50$  nm,  $n_0 = 3.35 \times 10^{12}$  vesicles/mL,  $|z_1| = |z_2| = 8980|e|$  (calculated by assuming that 20% of vesicle lipids are effectively charged), and  $\kappa^{-1} = 10$  nm, the numerical integration of the previous expression provides

$$G \approx 40 \text{ collisions/s}$$



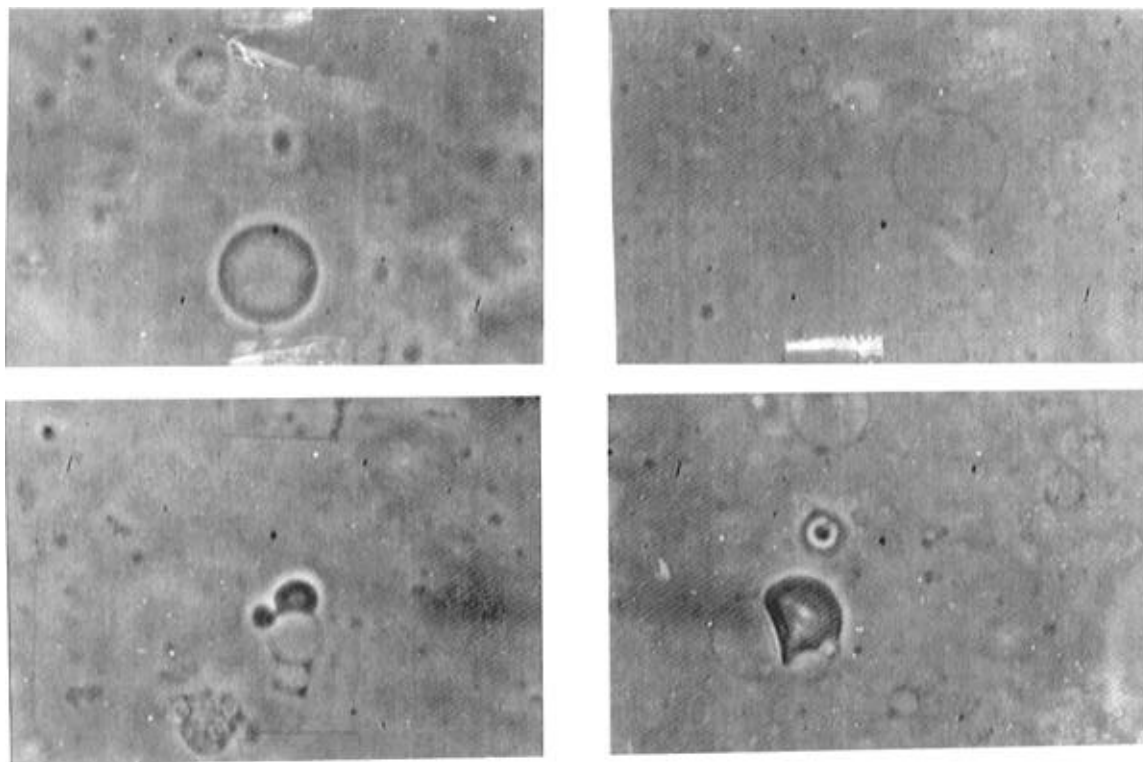


**Figure 8.** Photographs of giant vesicles as observed by phase contrast microscopy after contrast enhancement by appropriate dilution in a medium of intermediate refractive index: (top right) positively charged vesicles; (top left) negatively charged vesicles; (bottom) mixtures of positively and negatively charged vesicles. Scale: 1 cm = 19  $\mu$ m (see the Experimental Section).

Consequently, since a delay of about 1 min is introduced between the mixing of oppositely charged vesicles and the recording of the fluorescence spectra, it seems reasonable to assume that the equilibrium of lipid exchange can be reached if the scheme b of lipid exchange applies.

Is a factor  $10^2$ – $10^3$  for the kinetics of lipid exchange between vesicles bearing either opposite (less than 10 s) or identical (more than 1 h) surface charges compatible with scheme a? Studies related to determination of exit and entry rate constants for several compounds in micelles have demonstrated that exit was much slower than the corresponding entry, which was almost diffusion-controlled.<sup>48</sup> Consequently, it should essentially be the nature of the membrane where exchanging species are initially located that would control the rate of lipid exchange between vesicles. Therefore, the different behaviors of oppositely and identically charged vesicles can hardly be accounted for by mechanism a. In the case of mechanism b, this difference is explained by considering the repulsive energy required to bring into contact two lipid surfaces bearing charges of the same sign and the absence of a driving force for lipid exchange.

Another indication is provided by the shape of the titration curves in the presence of Rh-PE and TNS.<sup>52</sup> One can reasonably suppose that if mechanism a were operating, micelle-forming or water-soluble components would migrate from their vesicle of origin and would be shared among all the vesicles according to the corresponding partition coefficients related to the surface charges of the different vesicles.<sup>53</sup> As mentioned above, only stearylamine should be involved in this migration process, and in the course of the titration of positively charged vesicles by negatively charged ones, all the initially positive vesicles would remain positively charged before the equivalence point. The all or nothing behavior displayed in Figure 4 would thus imply sigmoidal titration curves for Rh-PE and TNS titrations: the fluorescence signal should vary essentially around the equivalence point but remain constant before and after equivalence.

In the present experiments, several titration curves strongly deviate from a sigmoidal character and can be satisfactorily described as linear before the equivalence point (Figure 5b). Such a linear behavior is best explained by mechanism b, for which lipid exchange occurs only between the two colliding vesicles (*vide infra*).

The final argument in favor of mechanism b was obtained from experiments with giant liposomes. Positively and negatively charged giant vesicles have been prepared<sup>54</sup> and observed by phase contrast microscopy by making use of refractive indexes of glucose/dextran solutions (Figure 8a,b). When mixtures of both vesicle preparations were observed, small aggregates of positive and negative vesicles were visible and were stable for more than 30 min (Figure 8c,d).

Lipid exchange is thus controlled by the contact between interacting vesicles. One should nevertheless be aware that our experiments do not address the precise mechanism when oppositely charged bilayers come into short range from each other. At this scale, it is possible that individual molecules or micelles are involved in the exchange process. Contact is to be taken in a broad sense.

**Final Surface Charges after Contact between Oppositely Charged Vesicles.** As a consequence of the preceding discussion, (i) the surface charges borne on bilayer surfaces in the vesicle populations during titration are necessarily heterogeneous, at least temporarily; and (ii) since the vesicle contact should preferentially involve the external leaflet, the surface charges on both leaflets in neutralized vesicles could be different just after the beginning of the lipid exchange process. The purpose of this paragraph is (i) to shed light on the heterogeneity of surface charge distribution among vesicles and within each vesicle during titration and (ii) to specify the extent of lipid exchange during the collision–adhesion events and the final surface charge of “neutralized” vesicles.

Considering first the fluorescence experiments, as discussed above, any mechanism leading to a homogenization of surface

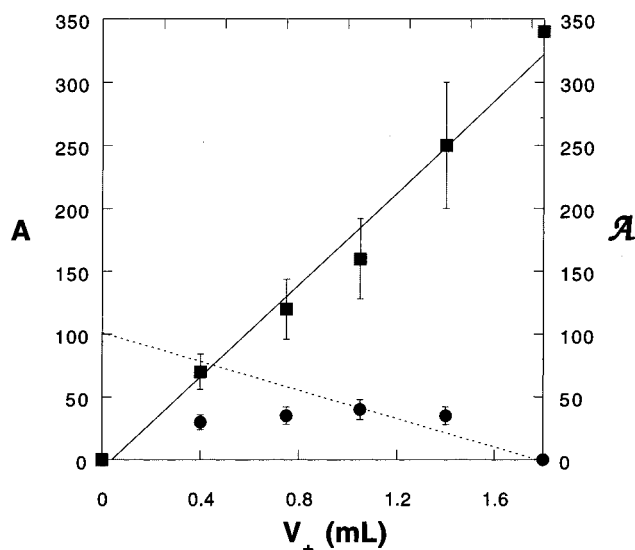


**Figure 9.** Normalized integrals  $A$  (markers; circles, -; squares, +) and calculated  $A$  integrals under the assumption of the absence of interaction between vesicles (lines; full line, +; dotted line, -) as a function of the volume  $V_+$  of positively charged vesicle suspension in the vesicle mixture (see Table 2).

charges would produce sigmoidal titration curves sensed by Rh-PE and TNS. The titration curve in Figure 5b being satisfactorily described as linear before the equivalence point, it seems that no homogenization of surface charge in the vesicle population occurs.

Information about the surface charge after lipid exchange between oppositely charged vesicles should be provided by examination of the fluorescence signal at equivalence under consideration of calibrations displayed in Figure 4. One difficulty consists here in extracting individual contributions from originally positively and negatively charged vesicles because the signal of the fluorescent probes expresses the behavior of the whole vesicle mixture. For experiments made at constant concentration of fluorescent probes (Figure 5b), the fluorescence beyond equivalence supports that vesicles bear reduced final surface charges at the end of the titration. In addition, the linear dependence of fluorescence signals for Rh-PE sensed titrations necessarily requires that the extent of exchange of charged lipid components during the adhesion event is almost complete (from 20% initial charged lipid to less than 1% remaining charge) in order to induce a significant change of fluorescence signal.

The preceding conclusions are supported by  $^{133}\text{Cs}$ -NMR experiments. In view of the absence of fusion and of the fluorescence observations related to the extent of exchange of charged lipid, the peak at 1.18 ppm has been first tentatively attributed to cesium cations contained in initially negatively charged vesicles that have been neutralized. The chemical shift calibration suggests that the corresponding internal concentration is less than 10 mM, a value departing significantly from the 20 mM initial concentration. The wall effect not explaining this discrepancy after the reduction of the charge surface of the leaflet to less than 1% in charged component, it seems reasonable to suppose that some leakage occurred during the washing step of the external vesicular medium.<sup>55</sup> After normalization on the peak corresponding to the external reference, integrals of the signals corresponding to positively charged vesicles ( $\delta = 1.71$  ppm),  $A_+$ , are linearly related to the volume,  $V_+$ , of positively charged vesicles initially present in the investigated mixtures (Table 2; Figure 9). The latter observation confirms the absence of vesicle fusion. In striking contrast, integrals  $A_-$  of the signals corresponding to initially

negatively charged vesicles ( $\delta = 1.18$  ppm) do not follow the linear behavior  $A_-$  calculated from the linear dependence of  $A_+$  by taking into account (i) the different experimental  $\text{Cs}^+$  concentrations in both vesicle populations and (ii) the expected difference in volumes of aqueous solution enclosed within vesicles because of the different vesicle diameters.<sup>56</sup>  $A_-$  displays a non-monotonous behavior, increasing almost linearly with  $V_-$  when positive lipids predominate among charged components within the mixture and then dropping when they become minor. This is precisely the expected behavior if only neutralized vesicles that were initially negatively charged were to display visible signals at 1.18 ppm because of a strong reduction of the charge of the membrane surface. Under these conditions, the ratio  $A_-/A_+$  would be identical to  $\inf(V_+, V_-)/V_-$ . This relation holds satisfactorily as shown on Table 3 and thus confirms the attribution of the 1.18 ppm peak to neutralize vesicles that were initially negatively charged.

The issue of lipid exchange between both leaflets in neutralized vesicles can also be addressed by  $^{133}\text{Cs}$ -NMR experiments. The preceding discussion directly shows that the internal vesicular surface is affected by the lipid exchange at the time scale required to prepare NMR samples. Such a fast change of lipid composition of the internal leaflet might result from some special lipid organization during vesicle contact. Nevertheless, a simple flip-flop of membrane components from or to the external leaflet would also account for the observed kinetics if one considers that (i) one-chain neutral lipids like stearylamine under their neutral form are expected to flip and flop at high rates and (ii) the selective neutralization of the external leaflet would create pH gradients across the membrane that are known to promote flip-flop translocation of pH active lipid components like stearylamine.<sup>57</sup>

As a conclusion, collisions between oppositely charged vesicles lead to a large exchange of charged components, strongly reducing the surface charges borne by both leaflets of bilayer vesicles.

**Significance of Vesicle Size for Lipid Exchange.** Vesicle size is expected to play a major role in the kinetics and thermodynamics of vesicle adhesion and lipid exchange. Two points will be successively addressed: (i) the evolution of the process rate when vesicular diameters are changed; and (ii) the significance of a difference in vesicular size between the positively and negatively charged vesicles.

Adhesion between giant liposomes has been observed for minutes, whereas it was impossible to detect any vesicle aggregates for experiments performed on DD LUVs. The explanation of this difference of behavior is based on the duration of lipid exchange. For LUVs, the value of the local charge density that is reached when interacting vesicles come into contact is smaller due to the smaller size of the charged component's reservoir so that the exchange duration is smaller. Moreover, the repulsive energetic term arising from deviation from the spherical shape when vesicles are stuck together<sup>6</sup> is larger in the LUV case.

The symmetrical titrations  $\text{Rh-/+}$  and  $\text{Rh+/-}$  displayed in Figure 5b,d exhibit a different behavior before equivalence. Whereas the titration curve is linear in the former case, it is sigmoidal in the latter. This dissymmetry can hardly be related to some specific property of the charged components that are contained within bilayers. The intrinsic  $\text{pK}_a$ 's of the amino or phosphatidic acid group are equally far from the used pH of aqueous solution.<sup>37</sup> The simplest explanation lies in the difference of diameters between positively and negatively charged vesicles. Since the collision between oppositely charged vesicles leads to a large exchange of lipids (*vide supra*),

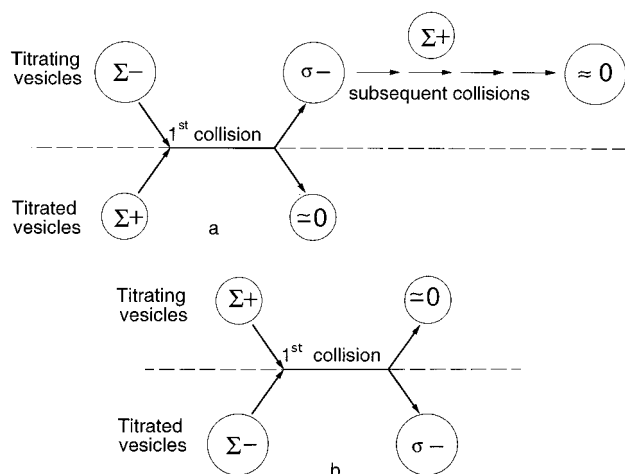


**Figure 10.** Neutralization mechanism of a titrating vesicle by vesicles of opposite charge. (a) titrating vesicles (surface charge  $\Sigma^-$ ) are the largest; (b) titrating vesicles (surface charge  $\Sigma^+$ ) are the smallest.

any difference of vesicle size at constant surface density of charged components implies the involvement of several encounters to "neutralize" the largest vesicles (negatively charged ones in the present case), whereas one encounter neutralizes the smallest ones. Before equivalence, two cases must be considered: (i) the titrating vesicles are the largest; the largest vesicles become neutral, whereas the smallest keep their initial sign of charge (Figure 10a); (ii) the titrating vesicles are the smallest; the smallest vesicle become neutral, whereas the largest keep their initial sign of charge (Figure 10b). Due to the Rh-PE dependence on the surface charge, the titration curve below equivalence is linear for the Rh-/+ titration (Figure 5b), whereas it will be more or less sigmoidal for the Rh+/- titration (Figure 5d).

Although appearing rather striking at first sight, the differences in behavior between large and giant vesicles for adhesion or between positively and negatively charged vesicles for lack of symmetry can be thus appropriately accounted for under consideration of differences in the size distribution of vesicle population.

**Nature of Exchanged Species.** By analyzing the evolution of surface charges, the preceding paragraphs cleared up the balance of charges during the lipid exchange process without addressing the nature of migrating molecules. In particular, in view of the expected differences in exit rates between neutral and charged one- or two-chain lipids in the presence of the electrical potential existing between interacting oppositely charged bilayers, one should reasonably suppose that one chain lipid charged components should be selectively extracted from interacting bilayers. In the present case, stearylamine would thus be the major migrating component. Nevertheless, some experimental results permit one to exclude the total absence of migration of other lipid components. First, upon consideration of the absence of vesicle aggregation and since NBD properties are not affected by pH nor by surface charge, it is necessary to suppose that some migration of NBD-PE or Rh-PE occurs besides the migration of stearylamine in order to account for the decrease of NBD fluorescence emission in the RET experiment displayed in Figure 1a. Similarly, the sole migration of stearylamine does not explain the non-monotonous evolution during -/Rh+ titration displayed in Figure 5c.<sup>58</sup>

## Conclusion

This study emphasizes some prominent features of vesicular systems. The dynamical structure of lipid media leads to

complex behavior. In the present system, the interaction between positively and negatively charged vesicles does not induce a permanent aggregation. Oppositely charged vesicles have been found to interact stepwise and to exchange lipid material without major structural reorganization. This process is shown to occur without fusion of internal vesicle pools. The size distribution of interacting vesicles plays a dramatic role in the rates of processes arising in mixtures. It is necessary to take into account the difference of size between interacting vesicles in order to interpret the often nonsymmetrical behavior arising from observation of symmetrical systems.

From an analytical point of view, the present study introduced two new tools for the investigation of vesicle interactions. Rh-PE was demonstrated to behave as a pH-sensitive probe of membrane surface charge in aqueous solutions of nonelectrolytes. On the other hand, <sup>133</sup>Cs-NMR has been shown to be a powerful technique for studying the behavior of vesicle mixtures. Since each population of vesicles exhibits a given NMR signal, it is possible simultaneously to investigate vesicle fusion, and membrane leakage or breakage and to separately follow the evolution of the internal surface charges of vesicular bilayer membranes.

The observation of fast lipid exchange bears much significance for drug targeting and delivery. The biological membrane surfaces being negatively charged, making use of electrostatic interaction appears an appealing way to favor exchange of membrane components if one can control the site of delivery. We are currently designing artificial systems to fulfill this task.

The overall process described here involves interaction and material exchange between polymolecular assemblies directed by effects of "electrostatic recognition" between their respective constituents. These aspects are also related to the more general question of "communication" (for instance via energy, electron, or ion transfer) between large polymolecular bodies on the basis of their supramolecular features.

## Experimental Section

**Materials.** Chemicals of the highest grade, cholesterol, *n*-octyl- $\beta$ -glucopyranoside, egg lecithin, stearylamine, and commercial standard positive and negative liposome kits were purchased from Sigma. The ternary liposome kits contain egg lecithin (70 mol %), cholesterol (10 mol %), and a third charged component CC (20 mol %), either stearylamine (positive kit) or dicetyl phosphate (negative kit). The fluorescent phospholipids *N*-(7-nitrobenz-2-oxa-1,3-diazol-4-yl)-1,2-dihexadecanoyl-*sn*-glycero-3-phosphoethanolamine, triethylammonium salt (NBD-PE), *N*-(Lissamine rhodamine B sulfonyl)-1,2-dihexadecanoyl-*sn*-glycero-3-phosphoethanolamine, triethylammonium salt (Rh-PE), and 2-(*p*-toluidinnaphthalene-6 sulfonic acid (TNS) were obtained from Molecular Probes. Calcein was purchased from Aldrich. The lipids were kept at  $-20^\circ\text{C}$  in chloroform solutions, and their purity was checked by TLC. The Britton-Robinson buffers at several pH and at 0.1 M ionic strength were prepared according to the literature.<sup>35</sup>

**Measurement of Osmotic Pressure.** Osmotic pressures of aqueous solutions were measured from determination of the temperature of liquid-vapor equilibrium with a Knauer osmometer. All external medium changes in vesicle suspensions were done under isoosmolar conditions.

**Vesicle Preparation.** Vesicles were prepared according to reported procedures.<sup>25</sup>

**Dialysis Method (DD).**<sup>29</sup> A chloroform solution of lipid components was evaporated under vacuum in a 50-mL round-bottomed flask at room temperature. A 10 molar equiv sample of *n*-octyl- $\beta$ -glucopyranoside and the appropriate volume of

aqueous solution were added to the resulting film. The mixture was vortexed until homogenization, and the resulting suspension of mixed micelles was dialyzed (dialysis bag Visking MW cutoff 12 000–10 000; Prolabo) against 1 L of aqueous solution for at least 5 h. This operation was repeated three times. Eventually, the preparation was filtered over Sephadex G-25 (PD-10 column, Pharmacia Biotech.; elution with the same aqueous solution as for the last dialysis). The preparations of positively charged vesicles prepared by this method were much less turbid than the corresponding preparations of negatively charged ones.

**Sonication.**<sup>30</sup> The chloroform solution of lipids was evaporated under vacuum at room temperature to produce a thin film on the walls of a small round-bottomed flask. After addition of aqueous solution, the suspension was continuously sonicated (Branson B 50 equipped with a titanium probe; 15 min; power 2, cooling at 0 °C). The preparation was then filtered on a short column of Sephadex G-25 M (Pharmacia PD-10, Pharmacia Biotech.; elution with the same aqueous solution as for the last dialysis).

**Reverse Phase Evaporation (REV).**<sup>31</sup> The chloroform lipid mixture (typically 10 mg) was added to a 50-mL round-bottomed flask, and the solvent was removed under reduced pressure at room temperature. Lipids were then redissolved in 3 mL of ether, and the aqueous solution (1 mL) was added. The resulting two-phase system was briefly sonicated (Branson B 50 equipped with a titanium probe; 3 min; power 2) while cooling at 0 °C until the mixture became a homogeneous opalescent dispersion, which did not separate after sonication for at least 30 min. The organic solvent was then removed under reduced pressure of nitrogen with a rotary evaporator to give first a viscous gel that subsequently transformed into an aqueous suspension. Vesicles were eventually sized successively on Nucleopore membranes of 5, 1, 0.8, 0.5, and 0.22  $\mu\text{m}$ .

**Giant Vesicles (GUV).**<sup>54</sup> A 15- $\mu\text{L}$  sample of lipid solution (1 mg/mL; solvent  $\text{CHCl}_3$ ) was deposited on two glass thin plates coated with a conducting film of fluorine-doped tin oxide. After drying for 30 min under nitrogen at room temperature, both glass plates were glued together with a Tygon tube 760  $\mu\text{m}$  in diameter as a spacer to build a cell with the conducting surfaces inside. An electric ac voltage (1 V, 10 Hz) was applied throughout this cell, and the appropriate aqueous solution was then injected at this point into the cell. Positively and negatively charged vesicles were swollen in aqueous solutions of different refractive index (negatively charged vesicles: glucose 10 mM, dextran 520 000 g/mol 7  $\mu\text{M}$ ; positively charged vesicles, glucose 10 mM). After mixing equal volumes of the preparations of both types of vesicles and by observation in the phase contrast mode of the microscope, both positively and negatively charged vesicles were differently contrasted.

**Characterization of Vesicles.** Two methods were used to determine lipid concentrations.

The lipid concentrations were first measured after mineralization. The amount of phosphate groups in a vesicular aliquot was estimated through phosphomolybdc complex formation and colorimetric determination.<sup>32</sup> Typically, for a vesicular preparation initially containing 3.4 mg of lipid mixture in 1 mL of aqueous solution, aliquots in the range 200  $\mu\text{L}$  were mineralized.

The determination of lipid composition, before and after vesicle preparation, and measurement of the yield of vesicle preparation were done by using a Iatroscan chromatography apparatus. Stock chloroform lipid solution (1  $\mu\text{L}$ ; concentration 10 mg/mL) were first prepared. In the case of vesicles, this solution was obtained after lyophilization of 2 mL of the vesicle suspension. Known amounts of these solutions were chromatographed on glass rods recovered by silica (eluting mixture:

chloroform/methanol/concentrated ammonia solution in water/water; 65/35/2.5/2.5 v/v). After elution, the rods were burnt and the detector provided the amount of each component of the lipid mixtures after a convenient calibration of pure individual components.

Along the present study, the number of equivalents  $\alpha$  used for titrations was defined as the ratio of the total amount of the potentially charged component (stearylamine or dicetyl phosphate) from the titrating solution to the total amount of the potentially charged component contained in the initial solution to be titrated.

**Spectroscopic Measurements. Absorption Spectra.** The UV–vis absorption spectra were recorded on a Beckmann DU 640 spectrophotometer with a slit width of 1 or 2 nm. Spectra were obtained by difference from a blank made of a suspension of nonlabeled vesicles. Typical lipid concentrations in samples for UV spectra were 3 mg/mL.

**Fluorescence Spectra.** Corrected fluorescence spectra were recorded on a Fluoromax SPEX fluorimeter with a slit width of 4 nm. All experiments were done with a sample absorbance at the wavelength of excitation inferior to 0.1. Vesicle solutions to be used for fluorescence experiments were prepared by convenient dilutions of initially concentrated vesicular solutions.

**Aqueous Contents Mixing. Terbium(III) Dipicolinate Assay.**<sup>40</sup> Positively and negatively charged vesicles were respectively prepared by dialysis (lipid concentration: 10 mg/mL) in isoosmolar (162 mOsM) aqueous solution obtained by suitable dilution with water from stock solutions: 2.5 mM  $\text{TbCl}_3$ , 50 mM citric acid, and 10 mM Tris base (positively charged vesicles) and 50 mM dipicolinate, 10 mM Tris, pH = 7 (negatively charged vesicles). Both vesicle solutions were extensively dialyzed against an isoosmolar solution of 150 mM glucose, 2 mM EDTA, and 10 mM Tris, pH = 7. The experiment consisted of monitoring the fluorescence emission ( $\lambda_{\text{exc}}$  = 286 nm;  $\lambda_{\text{em}}$  = 489, 542, or 582 nm) arising from Tb/DPA complex formation by mixing aliquots of solutions of positively and negatively charged vesicles. No fluorescence was detected in the course of these experiments.

**Cobalt(II) Calcein Assay.**<sup>41</sup> Positively charged vesicles (lipid concentration: 10 mg/mL) prepared by dialysis in 2 mM  $\text{CoCl}_2$ , 10 mM Tris, pH = 7, and 14 mM glucose and negatively charged vesicles (lipid concentration: 10 mg/mL) prepared by dialysis in 0.5 mM calcein, 8 mM Tris, pH = 7, 2 mM Tris base, and 20 mM glucose were dialyzed against an isoosmolar solution of 45 mM glucose. The experiment consisted of monitoring the quenching of calcein fluorescence ( $\lambda_{\text{exc}}$  = 490 nm;  $\lambda_{\text{em}}$  = 513 nm) corresponding to the Co/calcein complex formation when aliquots of solutions of positively and negatively charged vesicles were mixed. No fluorescence change was detected in the course of these experiments.

**NMR Measurements.** <sup>133</sup>Cs-NMR spectra were recorded at room temperature ( $20 \pm 2$  °C) on a Bruker AM 200 SY spectrometer operating at 26.25 MHz, using an external  $\text{D}_2\text{O}$  lock for field/frequency stabilization. Longitudinal relaxation times  $T_1$  were measured by the inversion recovery technique. The chemical shifts ( $\delta$ ) were given in ppm by using a 10.7 mM solution of  $\text{CsCl}$  in  $\text{D}_2\text{O}$  contained in a 10-mm NMR tube as an external reference. The samples of vesicular solutions in  $\text{H}_2\text{O}$  (1.8 mL) were poured into an 8-mm NMR tube, and the latter was introduced into the reference NMR tube 10 mm in diameter. Each sample was left for thermal equilibration for 15 min prior to measurement.

**Dynamic and Static Light Scattering.** Light scattering measurements were done at 20 °C on filtered vesicular solution (pore size: 0.25  $\mu\text{m}$ ) at several lipid concentrations. Incident

irradiation at 514.5 nm was produced by a coherent argon laser. A Brookhaven multi-autocorrelator was used to generate the full autocorrelation function of the scattered intensity. The time correlation function was analyzed by a method of cumulants. The static light scattering measurements were done between 50° and 130°. The values of gyration radii were extracted from the slope of the Guinier plots.

**Electron Microscopy.** Several conditions have been used for sample preparations. Frozen samples of concentrated vesicle suspensions in 10 mM glucose (lipid concentration range: 10–50 mg/mL) were prepared by the freeze–fracture technique either directly or after addition of 25% (v/v) glycerol as additional cryoprotector before sample freezing. Small droplets of vesicle suspensions were spread as a thick film between copper planchettes, and the sample was then rapidly frozen by plunging it into nitrogen at –210 °C under vacuum. The frozen specimens were fractured at 10<sup>–8</sup> Torr and –150 °C in a Reichert-Jung cryofract instrument. The fracture surfaces were replicated by evaporating 1.8 nm of platinum at 45° followed by 15 nm of carbon deposited normal to the fracture surface. Samples were brought to room temperature and atmospheric pressure and then cleaned in sodium hypochlorite aqueous solution to be eventually mounted on copper electron microscope grids observed at 80 kV with an EM 201 Philips electronic microscope.

**Acknowledgment.** Support of this work by a grant from L'OREAL is gratefully acknowledged. We are indebted to Florence Ricoul, Dr. Marie-Alice Guedeau-Boudeville, and Dr. Hubert Hervet for their kind help in the course of this study. Thierry Bataille is gratefully acknowledged for his contribution to the drawings.

**Supporting Information Available:** Size distribution of vesicles by electron microscopy and TNS fluorescence data (5 pages). Ordering information is given on any current masthead page.

## References and Notes

- (1) Abbreviations: CC, charged component; Chol, cholesterol; DOD-AB, dioctadecylammonium bromide; DPA, dipicolinic acid; EPC, egg yolk lecithin; LUV, large unilamellar vesicles; NBD-PE, *N*-(7-nitrobenz-2-oxa-1,3-diazol-4-yl) phosphatidylethanolamine; RET, resonance energy transfer; REV, vesicles prepared by the reverse phase method; Rh-PE, *N*-(Lissamine rhodamine B sulfonyl)phosphatidylethanolamine; TNS, 2-(*p*-toluidino)-naphthalene-6-sulfonic acid.
- (2) Hoppe, W.; Lohmann, W.; Markl, H.; Ziegler, H. *Biophysics*; Springer Verlag: Berlin, 1983.
- (3) Albert, B.; Bray, D.; Lewis, J.; Raff, M.; Roberts, K.; Watson, J. D. *Molecular Biology of the Cell*, 3rd ed.; Garland Publishing: New York, London, 1994.
- (4) Evans, E.; Needham, D. *J. Phys. Chem.* **1987**, *91*, 4219.
- (5) Chiruvolu, S.; Walker, S.; Israelachvili, J.; Schmitt, F. J.; Leckband, D.; Zasadzinski, J. A. *Science* **1994**, *264*, 1753.
- (6) Bailey, S. M.; Chiruvolu, S.; Israelachvili, J. N.; Zasadzinski, J. A. *Langmuir* **1990**, *6*, 1326.
- (7) Kimizuka, N.; Kurihara, K.; Kunitake, T. *J. Am. Chem. Soc.* **1993**, *115*, 4387.
- (8) Israelachvili, J. *Intermolecular and Surface Forces*; 2nd ed.; Academic Press: London, San Diego, New York, Boston, Sydney, Tokyo, Toronto, 1991.
- (9) Pincet, F.; Perez, E.; Bryant, G.; Lebeau, L.; Mioskowski, C. *Phys. Rev. Lett.* **1994**, *73*, 2780. Pincet, F.; Perez, E.; Lebeau, L.; Mioskowski, C. *J. Chem. Soc., Faraday Trans.* **1995**, *91*, 4329.
- (10) Ikeura, Y.; Kurihara, K.; Kunitake, T. *J. Am. Chem. Soc.* **1991**, *113*, 7342.
- (11) Ahuja, R.; Lorenzo Casuro, P.; Möbius, D.; Paulus, W.; Ringsdorf, H.; Wildburg, G. *Angew. Chem., Int. Ed. Engl.* **1993**, *105*, 1082.
- (12) Ringsdorf, H.; Schlarb, B.; Venzmer, J. *Angew. Chem., Int. Ed. Engl.* **1988**, *27*, 113.
- (13) Ahlers, M.; Müller, W.; Reichert, A.; Ringsdorf, H.; Venzmer, J. *Angew. Chem., Int. Ed. Engl.* **1990**, *29*, 1269.
- (14) Schneider, H.-J. *Angew. Chem., Int. Ed. Engl.* **1991**, *30*, 1417.
- (15) Fendler, J. H. *Membrane Mimetic Chemistry*; Wiley: Chichester, 1982.
- (16) Lasic, D. D. *Liposomes from Physics to Applications*; Elsevier: Amsterdam, 1993.
- (17) Lätiger, P. *Angew. Chem., Int. Ed. Engl.* **1988**, *24*, 905.
- (18) Döbereiner, H.-G.; Käs, J.; Noppl, D.; Sprenger, J.; Sackmann, E. *Biophys. J.* **1993**, *65*, 1396.
- (19) Menger, F. M.; Gabrielson, K. D. *Angew. Chem., Int. Ed. Engl.* **1995**, *34*, 2091.
- (20) Gregoriadis, G. *Liposome Technology*; CRC: Boca Raton, FL, 1984.
- (21) Castaing, M.; Morel, F.; Lehn, J.-M. *J. Membr. Biol.* **1986**, *89*, 251.
- (22) Pregel, M.; Jullien, L.; Canceill, J.; Lacombe, L.; Lehn, J.-M. *J. Chem. Soc., Perkin Trans. 2* **1995**, 417.
- (23) Stamatatos, L.; Leventis, R.; Zuckermann, M. J.; Silvius, J. R. *Biochemistry* **1988**, *27*, 3917.
- (24) Thomas, R. C.; Houston, J. E.; Crooks, R. M.; Kim, T.; Michalske, T. A. *J. Am. Chem. Soc.* **1995**, *117*, 3830.
- (25) *Liposomes, A Practical Approach*; New, R. R. C., Ed.; Oxford University Press: New York, 1990.
- (26) Carmona-Ribeiro, A. M.; Castuma, C. E.; Sesso, A.; Schreier, S. *J. Phys. Chem.* **1991**, *95*, 5361 and references therein.
- (27) Rupert, L. A. M.; Hoekstra, D.; Engberts, J. B. F. N. *J. Colloid Interface Sci.* **1987**, *120*, 125; *Biochim. Biophys. Acta* **1995**, *1241*, 323.
- (28) Cuccovia, I. M.; Feitosa, E.; Chaimovich, H.; Sepulveda, L.; Reed, W. J. *J. Phys. Chem.* **1990**, *94*, 3722.
- (29) Mimms, L. T.; Zampighi, G.; Nozaki, Y.; Tanford, Reynolds, J. A. *Biochemistry* **1981**, *20*, 833.
- (30) Milon, A.; Lazrak, T.; Albrecht, A. M.; Wolff, G.; Weill, G.; Ourisson, G.; Nakatani, Y. *Biochim. Biophys. Acta* **1986**, *859*, 1.
- (31) Szoka, F., Jr.; Papahadjopoulos, D. *Proc. Natl. Acad. Sci. U.S.A.* **1978**, *75*, 4194.
- (32) Chen, P. S., Jr.; Toribara, T. Y.; Warner, H. *Anal. Chem.* **1956**, *28*, 1756. Morrison, W. R. *Anal. Biochem.* **1964**, *7*, 218.
- (33) Hoekstra, D.; Düzgünes, N. *Methods Enzymol.* **1993**, *220*, 15.
- (34)  $\alpha$  was introduced as a measure of the titration extent. Initially,  $\alpha = 0$ , and at equivalence,  $\alpha = 1$ .
- (35) Frugoni, C. *Gazz. Chim. Ital.* **1957**, *87*, 403.
- (36) A relatively high ionic strength ensures that the pH sensed close to charged membrane surfaces is similar to the pH in the bulk solution.
- (37) Perrin, D. D. *Dissociation Constants of Organic Bases in Aqueous Solution: Supplement 1972*; Butterworths: London, 1972. Kortüm, G.; Vogel, W.; Andrusow, K. *Dissociation Constants of Organic Acids in Aqueous Solution*; Butterworths: London, 1961. Albert, A.; Serjeant, E. P. *Ionization Constants of Acids and Bases*; Methuen & Co.: London; John Wiley & Sons Inc.: New York, 1962.
- (38) This simulation is based on emission measured after addition of aliquots of Rh-PE-containing vesicles to isoosmolar glucose solutions.
- (39) Langner, M.; Cafiso, D.; Marcelja, S.; McLaughlin, S. *Biophys. J.* **1990**, *57*, 335.
- (40) Ellens, H.; Bentz, J.; Szoka, F. C. *Biochemistry* **1985**, *24*, 3099.
- (41) Kendall, D. A.; McDonald, R. *Anal. Biochem.* **1983**, *134*, 26.
- (42) Rymden, R.; Jansson, M.; Edwards, K.; Almgren, M.; Brown, W. J. *Colloid Interface Sci.* **1989**, *128*, 477.
- (43) Jullien, L.; Lazrak, T.; Canceill, J.; Lacombe, L.; Lehn, J.-M. *J. Chem. Soc., Perkin Trans. 2* **1993**, 1011 and references therein.
- (44) Brévard, C.; Granger, P. *Handbook of High Resolution Multinuclear NMR*; John Wiley and Sons: New York, 1981.
- (45) Mei, E.; Dye, J. L.; Popov, A. J. *Am. Chem. Soc.* **1977**, *99*, 5308.
- (46) Jullien, L.; Marchi-Artzner, V.; Fosset, B.; Belloni, L.; Lacombe, L.; Lehn, J.-M. To be submitted.
- (47) By taking into account average vesicular diameters and the respective internal cesium concentrations of initially negatively and positively charged vesicles, one should expect by fusion a new NMR peak at about 1.4 ppm. For the purpose of clarity, the interpretation of the peak at 1.18 ppm will be given in the following paragraphs.
- (48) Zana, R. In *Surfactant Solutions: New Methods of Investigation*; Zana, R., Ed.; Marcel Dekker Inc.: New York, 1987.
- (49) Pagano, R. E.; Martin, O. C.; Schroit, A. J.; Struck, D. K. *Biochemistry* **1981**, *20*, 4920. Struck, D. K.; Hoekstra, D.; Pagano, R. E. *Biochemistry* **1981**, *20*, 4093.
- (50) Some remaining detergent should have played a role in the exchange process. In fact, we did not detect any significant amount of octylglucopyranoside, if any, during analysis of membrane composition. Furthermore, we reproduced Rh-PE and TNS titrations with REV prepared in the absence of detergent and DD LUV-like observations were made.
- (51) Verwey, E. J. W.; Overbeek, J. Th. G. *Theory of the Stability of Lyophobic Colloids*; Elsevier: New York, 1948.
- (52) The following discussion assumes that fluorescent probes do not induce any change of the mechanism of vesicle interaction. All experiments are thus expected to provide a coherent picture.

(53) Reported results on PE fluorescent probes suggest that the surface charge of bilayers does not introduce dramatic changes of partition coefficients. See: Nichols, J. W.; Pagano, R. E. *Biochemistry* **1982**, *21*, 1720.

(54) Angelova, M. I.; Dimitrov, D. S. *Mol. Cryst. Liq. Cryst.* **1987**, *152*, 89.

(55) Indeed, phosphate lipids are expected to transport cations through bilayers by flip-flop of the neutral ion pair. The difference in behavior between positively and negatively charged vesicles in the leakage rate is explained since it is known that cation exit constitutes the rate-limiting step of passive leakage of salts contained in vesicles.

(56) The ratio of compartmented volumes is proportional to the ratio of vesicle diameters since lipid concentrations and vesicle structures are

identical for both populations of vesicles.

(57) Cribier, S.; Devaux, P.; Mathivet, L. Private communication on pH-induced morphological changes of giant liposomes.

(58) The decreasing branch of the titration curve is explained by considering that already one-time neutralized vesicles become neutral after subsequent collisions with the positively charged titrating vesicles. Figure 4 suggests the Rh-PE fluorescence emission in EPC or negatively charged vesicles to be similar. Nevertheless, one cannot exclude some marginal EPC hydrolysis to yield a negatively charged surface. In a true neutral environment, Rh-PE should give an intermediate signal between positively and negatively charged vesicles.

JP960327F